IDyLL: Indoor Localization using Inertial and Light Sensors on Smartphones

Conference Paper · September 2015

DOI: 10.1145/2750858.2807540

3 authors, including:

Rong Zheng
McMaster University
164 PUBLICATIONS **2,140** CITATIONS

SEE PROFILE

IDyLL: Indoor Localization using Inertial and Light Sensors on Smartphones

Qiang Xu
Department of Computing and Software
McMaster University
1280 Main St. W., Hamilton, ON, Canada
xuq22@mcmaster.ca

Rong Zheng
Department of Computing and Software
McMaster University
1280 Main St. W., Hamilton, ON, Canada
rzheng@mcmaster.ca

Steve Hranilovic
Department of Electrical & Computer Engineering
McMaster University
1280 Main St. W., Hamilton, ON, Canada
hranilovic@mcmaster.ca

ABSTRACT

Location-based services have experienced substantial growth in the last decade. However, despite extensive research efforts, sub-meter location accuracy with low-cost infrastructure continues to be elusive. In this paper, we propose IDyLL – an indoor localization system using inertial measurement units (IMU) and photodiode sensors on smartphones. Using a novel illumination peak detection algorithm, IDyLL augments IMU-based pedestrian dead reckoning with location fixes. We devise a robust particle filter framework to mitigate identity ambiguity due to the lack of communication capability of *conventional* luminaries and sensing errors. Experimental study using data collected from smartphones shows that IDyLL is able to achieve high localization accuracy at low costs. Mean location errors of 0.38 m, 0.42 m, and 0.74 m are reported from multiple walks in three buildings with different luminary arrangements, respectively.

ACM Classification Keywords

C.3.3 SPECIAL-PURPOSE AND APPLICATION-BASED SYSTEMS: Real-time and embedded systems

Author Keywords

Indoor localization; Peak detection; Particle filter; conventional luminary;

INTRODUCTION

Location-based services (LBS) have experienced substantial growth in the last decade with the proliferation of smart devices. A recent survey by Pew Research Center's Internet Project found that 74% of adult smartphone owners aged 18 and older use their phone to get directions or other information based on their current location [1]. Service providers can benefit from users' location information in facilitating precision advertising, personalized recommendation, resource tracking and proximity notification, etc. For example, social media sites use location information to notify people who and what is near them as a means to attract more users.

To provide LBS, location awareness is an essential step. The Global Positioning System (GPS) complimented by cellular and WiFi access map based methods [36, 33] can provide accurate and robust location information in most outdoor environments. In contrast, despite the fact that people spend majority of their time indoor, indoor positioning systems (IPS) only have limited success due to low accuracy. Conventional GPS signals are highly attenuated indoor rendering GPS-based position estimates inaccurate. The main challenges in IPS arise from the lack of pervasive infrastructural support, and the desire to keep user devices as simple as possible.

In this work, we explore an often overlooked but pervasive source of information in indoor environments for localization, namely, luminaries (including incandescent, fluorescent and LED luminaries, etc.). For instance, a single floor of the 83m×73m building at the authors' workplace features 116 luminaries along the corridor alone. In order to provide appropriate illumination, these luminaries are generally evenly spaced except at corners and entrance areas. Many models of smartphones and wearable devices already feature light sensors (photodiodes) for automatic brightness adjustment, including Google glass, Nexus 4, Nexus 5, Nexus 7, iPhone, Pebble, etc. Though some of the built-in light sensors can theoretically sample at a high rate (e.g., 1.17MHz for APDS-9303 on Nexus 5 and 7), they are often constrained either by the hardware interface or the OS-level support to a few Hz to up to 100Hz. Such a low sampling rate makes these sensors unsuitable to decode data for visible light communication (VLC) and visible light positioning (VLP) that typically require a sample rate of multiple kHz or higher. However, we show that they can still be utilized to extract useful location information.

Utilizing luminaries and photodiodes on smartphones for IPS faces several challenges. Firstly, luminaries may be dimmed or the brightness of luminaries may vary depending their age. Secondly, depending on the orientation of the device, the intensity measured by the photodiodes also changes. Thirdly, despite the fact that luminary locations are typically fixed and can be obtained either through building management or a one-time site survey, luminaries may burn out or shutoff during maintenance. Lastly and most importantly, due to the lack of communication capabilities on the luminaries and the sensors,

UbiComp '15, September 7-11, 2015, Osaka, Japan.

http://dx.doi.org/10.1145/2750858.2807540

the exact identity of a luminary can not be reliably determined. Such an identity ambiguity translates to location uncertainty especially when luminaries are evenly spaced.

In this paper, we propose IDyLL, an indoor localization system using existing inertial and light sensors on smartphones and wearable devices. IDyLL does not require additional infrastructure support or device modification beyond what are currently available. It is the first system that exploits *conventional* indoor luminaries for fine-grained indoor localization and demonstrates their usefulness experimentally. To address the afore-mentioned challenges, we devise robust algorithms both at the component level and at the system level. At the component level, detection of luminaries is based on variations (e.g., presence of a peak) in illumination intensity as people move around indoor environments rather than absolute intensity readings. To mitigate motion estimation errors from IMU sensors, we utilize past estimates of moving speed (rather than step counts). To alleviate the uncertainty in stride length, spacing of luminaries is utilized. At the system level, we incorporate in a particle filter framework that explicitly models sensing errors.

Evaluation of IPS solutions is known to be labor-intensive and prone to errors. The data collection system we devise utilizes a head-mounted camera to record marker locations and footsteps, and a mobile phone that records IMU data. Time synchronization across devices is achieved via audio cues generated by the phone. The recorded video is then post-processed offline to extract ground truth locations and step counts. Experimental study using data collected from smartphones shows that IDyLL is able to achieve high localization accuracy at low costs. Mean location errors of 0.38 m, 0.42 m and 0.74 m are reported for multiple walks in three buildings with different luminary arrangements in presence of luminaries burnt out, respectively.

It should be noted that IDyLL builds upon existing work on pedestrian dead reckoning (PDR) (*e.g.* [5, 9]). The main contribution of IDyLL lies in novel mechanisms *i) to include conventional illumination information in both motion and observation models, and ii) to robustly fuse multiple sensory data in a rigorous framework*.

The rest of this paper is organized as follows. In the related work section, some relevant prior work in IPS is discussed. Next, we give a high level description of IDyLL followed by the theoretical framework of particle filter in indoor localization. Details are provided on algorithms for deriving the motion model and observation model from sensing data, respectively. Experimental results are presented and are followed by discussion of the limitations of IDyLL. Finally, we conclude the paper with directions for future work.

RELATED WORK

Indoor localization has received much attention in recent years. Existing solutions to indoor positioning mainly fall into two categories: device-based and device-free. Among device-based approaches, various signals including ultra-wide-band RF signals, WiFi signals, acoustic or the combination of them can be used to derive range [21], pseudo-range [19], angle-of-arrival [29], or proximity [3]. However, these approaches either rely on costly infrastructure, require modification to end user devices or fail to achieve satisfactory positioning accuracy.

PDR utilizing IMUs on smartphones or wearable devices has been investigated in several work [16, 14, 15, 23] for indoor localization. A comprehensive survey paper on PDR can be found in [10]. Most IMU-based IPS have the following components i) step counting, ii) stride length estimation, iii) heading estimation, and iv) a particle filter. Existing approaches differ in the type and position of sensors placed on body, preprocessing procedure of sensor data, and whether backtracking is employed, etc. Prior knowledge of the map can help alleviate the error accumulation in PDR systems. As pointed out by [16, 2], PDR techniques alone can offer good short- to medium-term tracking under certain circumstances, but regular absolute position fixes will be needed to ensure long-term operation and to cope with unexpected behaviors. Location fixes can be provided using WiFi, acoustic, magnetic or optical landmarks.

Little work has been done to leverage information from unmodified luminaries in indoor localization. In [8, 24], the authors assume that the illumination intensity and ambient colour vary from room to room and thus can be used as fingerprints for room-level localization. Collection of illumination fingerprints is cumbersome and potentially unreliable as ambient illumination varies over time. Closest to our approach is the work called Light-matching by Jimenez *et al.* [12]. Light-matching utilizes position, orientation and shape information of all indoor luminaries, and models illumination intensity using an inverse-square law. To distinguish different luminaries, it relies on asymmetries/irregularities of luminary placement. We find through our experiments that in many environments luminaries are in fact often evenly distributed. Furthermore, evaluation for Light-matching in [12] is only done via simulation, and thus its performance in real-world settings remains unknown.

Several approaches to localization using *modulated* luminaries have been proposed. Most techniques employ received intensity measurements to extract position information from multiple transmitters using a suitable channel model. Absolute and relative intensity measurements for localization have been proposed in [34, 13], respectively, both work requiring knowledge of the receiver orientation to solve for a position. The use of a receiver with a 6-axis IMU to provide this orientation information has been proposed in [26]. An inherent weakness of these intensity measurement approaches is that they all require accurate knowledge of both the output power and spatial characteristics of each transmitter. The luminous intensities of LEDs in a luminary can vary with process variations, temperature and device age. Additionally, assuming a Lambertian radiation pattern from a luminary is often inaccurate when collimating or diffusing optics are used to achieve uniform illumination [28]. Thus, calibration is a requirement of intensity measurement techniques. A coarse positioning algorithm which partially avoids this problem by using a binary weighting scheme applied to identifiable luminaries has been proposed in [22]. Localization using imaging techniques

measures geometric relations between luminaries instead of channel measurements [32]. This method suffers from the same orientation issues as other approaches, and fast drains the battery of the device. Notice that all previous approaches require multiple transmitters to be simultaneously within the receiver field-of-view (FOV). Another approach exploits the directionality of free space optics where angular information is encoded by discrete emitters [4]. In Epsilon and Pharos [17, 11], sub-meter localization errors are reported by using modulated LEDs as location beacons.

IDyLL differs from VLP in its ability to exploit *conventional* luminary infrastructure and does not require extra hardware supports on consumer devices. IDyLL leverages and augments PDR techniques with illumination peak detection, which can provide a level of location fix. However, due to identity uncertainty discussed in the introduction, the resulting location fixes may have some ambiguity in themselves. The main contributions of this paper are summarized as follows:

- **New sensing modality:** IDyLL takes advantage of prevalent indoor lighting structure and photodiode sensors on smart phones in location estimation.
- **Luminary-assisted displacement estimation:** IDyLL uses adaptive filters to extract heading and step counts from IMU data. The distances between neighboring luminaries are utilized to enhance stride length estimation.
- **Design of an evaluation platform for IPS:** IDyLL automates the process of data acquisition and ground truth extraction.

SYSTEM ARCHITECTURE

In this paper, we consider the scenario where a pedestrian moving inside a building while holding a mobile device face-up for navigation. The floor map and luminary placement are known. The initial location is assumed to be known and could be obtained using a GPS fix when she enters the building or by manual input.

The overall architecture of IDyLL is illustrated in Figure 1. IDyLL utilizes IMU and light sensors on smartphones. The sampling rates of the IMU and light sensors are 200Hz and 10Hz, respectively. The accelerometer data is pre-processed by an adaptive filter for step detection. The estimated step frequency is then incorporated in a stride length estimation module, which together with step counts provide an estimation of the user's speed. Heading is estimated by a complementary filter combining readings from both the compass and the gyroscope.

As discussed in the introduction, illumination intensity levels measured on a phone tend to vary as a result of factors such as luminary aging, orientation of photodiodes, distance, etc. IDyLL does not use absolute intensity readings. Instead, peak detection is employed to help infer the trajectory when the user is under a luminary. Here, we assume non-uniform lighting conditions and that the illumination intensity decreases as the user moves away from the light source. Figure 2 shows the raw data from the light sensor when a user moves along the hallway of two buildings. The luminary arrangement is shown in Figure 3(a)(b) in the two settings. We can clearly identify the peaks from Figure 2 despite the relative low sampling rate. Using step counts and the knowledge of luminary spacing, frequency-based stride length estimation can be further refined.

A particle filter is then devised given the motion model (i.e., the velocity and heading), the observation model (i.e., illumination peaks), and map knowledge. At each time instance, the particle filter outputs a weighted point cloud for the candidate locations. We take its centroid as the estimated user location.

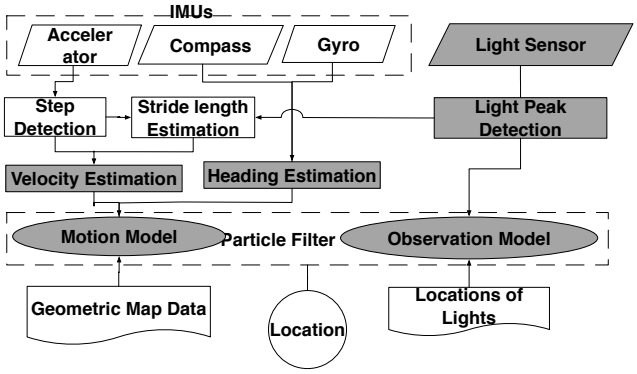

Figure 1. The System Architecture of IDyLL

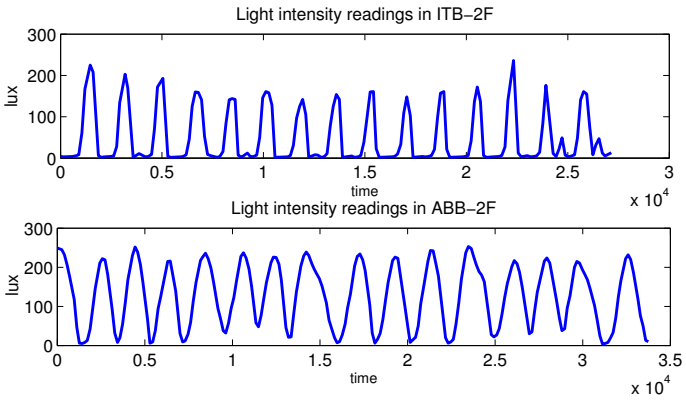

Figure 2. The Illumination Intensity in Two Different Settings

(a) ITB-2F (b) ABB-2F (c) MUSC-3F

Figure 3. Different Light Arrangements in Three Buildings

BAYESIAN FILTERING FOR INDOOR LOCALIZATION

System model and Bayesian predictive inference

Bayesian filters can estimate the evolution of the probability density function of the true states of a dynamic system from noisy observations. Adopting the terminologies in [7, 6, 9], the evolution of the system is confined to discrete times $\langle t_0, ..., t_k \rangle$ where $t_k = t_{k-1} + T_{k-1}$, t_k is the kth time stamp and T_k is the kth interval.

The hidden states $\{\vec{s}_t; t \in \mathbb{N}\}$ are modeled as a Markov process where $\vec{s}_t \in \mathbb{R}^m$ is an m-dimensional random variable indicating the unobserved state at time t. In the current implementation of IDyLL, $m = 2$ and $\vec{s}_t = (x_t, y_t)$ are associated with 2-D coordinates. The given prior map information is $\mathscr{M} = (\mathscr{M}_p, \mathscr{M}_l)$, where $\mathscr{M}_p$ and $\mathscr{M}_l$ are respectively, the floor map and the luminary placement map. The initial distribution of $\vec{s}$ is $f_0(\vec{s})$, and the transition probability density function is given by $f_t(\vec{s}_t|\vec{s}_{t-1}, \mathscr{M})$ (called *the motion model*). The observations are $\{o_t, t \in \mathbb{N}\}$ where o_t is the *binary* observation whether an illumination peak is detected at time t. We assume that o_t's are conditionally independent given $\{\vec{s}_t; t \in \mathbb{N}\}$ with a marginal distribution $p(o_t|\vec{s}_t)$ (called *the observation model*). Therefore, the complete system model can be described as:

$$\begin{aligned} f_0(\vec{s}_0|\mathscr{M}) \\ f_t(\vec{s}_t|\vec{s}_{t-1}, \mathscr{M}) \\ p(o_t|\vec{s}_t, \mathscr{M}) \end{aligned} \tag{1}$$

The system state $\vec{s}_t$ depends on all past observations $o_{0:t} = \{o_0, ..., o_t\}$. Our aim is to estimate the marginal posterior distributions $p(\vec{s}_t|o_{0:t}, \mathscr{M})$ and its expectation $I(\vec{s}_t)$, recursively. This recursion can be divided into two steps, namely, prediction and updating.

Prediction

The next system state $p(\vec{s}_t|o_{0:t-1})$ is predicted using the prior distribution $p(\vec{s}_{t-1}|o_{0:t-1})$ and the transition probability density function $f_t(\vec{s}_t|\vec{s}_{t-1})$,

$$p(\vec{s}_t|o_{0:t-1}, \mathscr{M}) = \int f_t(\vec{s}_t|\vec{s}_{t-1}, \mathscr{M}) p(\vec{s}_{t-1}|o_{0:t-1}, \mathscr{M}) d\vec{s}_{t-1}. \tag{2}$$

Updating

The proposal distribution $p(\vec{s}_t|o_{0:t-1}, \mathscr{M})$ is updated using the new measurement o_t yielding $p(\vec{s}_t|o_{0:t}, \mathscr{M})$,

$$p(\vec{s}_t|o_{0:t}, \mathscr{M}) = \frac{p(o_t|\vec{s}_t, \mathscr{M}) p(\vec{s}_t|o_{0:t-1}, \mathscr{M})}{\int p(o_t|\vec{s}_t) p(\vec{s}_t|o_{0:t-1}, \mathscr{M}) d\vec{s}_t}. \tag{3}$$

(2) and (3) form the basis of Bayesian Predictive Inference. They are deceptively simple without considering the normalizing constant $p(o_{0:t})$. However, the marginal posterior distribution $p(\vec{s}_t|o_t)$ cannot be computed straightforwardly since the computation requires complex high-dimensional integrals [6].

Sampling importance resampling filter (bootstrap filter)

It is generally difficult to obtain a closed-form solution to the expectation of the marginal posterior distribution using the recursive steps of Bayesian predictive inference. Instead, sequential Monte Carlo sampling based methods are often adopted [6, 9, 7]. In this section, we introduce a special Bayesian filter – Sequential Importance Resampling (SIR) Particle Filter, also known as *Bootstrap Filter*. To help understand Bootstrap Filter, let us first introduce Importance Sampling (IS). Importance sampling, a fundamental Monte Carlo method, is widely used to sample from high- dimensional probability distributions. In the IS method, a so-called *importance sampling distribution* $\pi(\vec{s}_t|o_{0:t})$ is used to calculate the expectation of the marginal posterior distribution as:

$$I(\vec{s}_t) = \frac{\int \vec{s}_t w(\vec{s}_t) \pi(\vec{s}_t|o_{0:t}) d\vec{s}_t}{\int w(\vec{s}_t) \pi(\vec{s}_t|o_{0:t}) d\vec{s}_t}, \tag{4}$$

where $w(\vec{s}_t) = \frac{p(\vec{s}_t|o_{0:t})}{\pi(\vec{s}_t|o_{0:t})}$ is known as the importance weight. As a result, if N i.i.d. particles are simulated, the expectation can be estimated as $\hat{I}_N(\vec{s}_t) = \sum_{i=1}^{N} \vec{s}_t^{(i)} \tilde{w}_t^{(i)}$, where $\tilde{w}_t^{(i)}$ is the normalized importance weight. To estimate the evolution of the system recursively using (1), IS is modified to the Sequential Importance Sampling (SIS). In SIS, $\pi(\vec{s}_t|o_{0:t}) = \pi(\vec{s}_{t-1}|o_{0:t-1}) \pi(\vec{s}_t|\vec{s}_{t-1}, o_{0:t}) = \pi(\vec{s}_0) \prod_{k=1}^{t} \pi(\vec{s}_k|\vec{s}_{k-1}, o_{1:k})$. If we adopt the prior distribution as the importance distribution:

$$\pi(\vec{s}_t|o_{0:t}) = f_0(\vec{s}) \prod_{k=1}^{t} f_k(\vec{s}_k|\vec{s}_{k-1}) \tag{5}$$

Then the importance weight satisfy

$$\tilde{w}_t^{(i)} \propto \tilde{w}_{t-1}^{(i)} p(o_t|\vec{s}_t^{(i)}) \tag{6}$$

Although SIS is attractive, as t increases, the distribution of importance weight will be skewed [6]. An additional selection of $\tilde{w}_t^{(i)}$ (Resampling) is introduced to resolve this problem. The key idea of resampling is that in every iteration we select $\vec{s}_t^{(i)}$ with probability $\tilde{w}_t^{(i)}$. SIS and Resampling comprise the Sampling Importance Resampling Filter (SIR). The SIR filter performs Sequential Monte Carlo estimation and uses a set of weighted particles $\{\langle \vec{s}_t^{(i)}, w_t^{(i)} \rangle, i = 1, ..., N\}$ to represent the posterior distribution $p(\vec{s}_t|o_{0:t})$.

Let $\{\langle \vec{s}_0^{(i)}, w_0^{(i)} \rangle, i = 1, ..., N\}$ be the initial set of particles representing the known prior probability density of the system's initial state $f_0(\vec{s})$. The recursion can be rewritten as:

Step 1. Prediction

The transition probability density function $f(\vec{s}_t|\vec{s}_{t-1}, \mathscr{M})$ is sampled to generate a new particle from each old particle. Some particles may disappear when the corresponding density is zero (e.g., due to map constraint). The total number of particles N' may be less than N after transition.

$$\langle \vec{s}_{t-1}^{(i)}, w_{t-1}^{(i)} \rangle \xrightarrow{\text{Motion Model}} \langle \vec{s}_t^{(i)}, w_{t-1}^{(i)} \rangle, \tag{7}$$

The current location of the user can be estimated using the expectation $\hat{I}_N = \sum_{i=1}^{N} \vec{s}_t^{(i)} w_{t-1}^{(i)}$.

Step 2. Updating

Given the observation probability $p(o_t|\vec{s}_t)$, the importance weight can be updated according to (6). $\{\langle \vec{s}_t^{(i)}, \tilde{w}_t^{(i)} \rangle, i =$

$1,...,N'\}$ describes the updated estimation of the state distribution $p(\vec{s}_t|o_{0:t})$ at time t with the addition of the new observation o_t.

Step 3. Resampling

Resampling is used to avoid the degeneration of SIS. The basic idea is to sample the final distribution $\{\langle \vec{s}_t^{(i)}, w_t^{(i)} \rangle, i = 1,...,N\}$ from $\{\langle \tilde{\vec{s}}_t^{(i)}, \tilde{w}_t^{(i)} \rangle, i = 1,...,N'\}$ such that $w_t^{(i)} = 1/N$.

$$\{\langle \tilde{\vec{s}}_t^{(i)}, \tilde{w}_t^{(i)} \rangle\} \xrightarrow{\text{Resampling}} \{\langle \vec{s}_t^{(i)}, 1/N \rangle\} \tag{8}$$

To reduce the computation complexity, we adopt the adaptive resampling method in [7] to carry out the resampling step only when the effective sample size (ESS) drops below a certain threshold. ESS is measured by

$$\text{ESS} = \left(\sum_{i=1}^{N} (\tilde{w}_t^{(i)})^2 \right)^{-1} \tag{9}$$

In the implementation, we choose the threshold to be $N/2$.

To this end, we have discussed how to perform SIR in the particle filter framework. In the next two sections, we derive the observation and motion models based on light and IMU sensor measurements. Note that the framework is extensible to other types of sensing modalities.

PEAK ILLUMINATION INTENSITY AS OBSERVATIONS

IDyLL exploits the variation in illumination intensity as users move around in indoor environments. We observe sharp peaks as one approaching a luminary and moving away. Presence of the peaks embeds location information.

Peak extraction

Let the samples collected from the phone photodiode be $z(t)$. The goal of peak illumination extraction is to identify and extract the timing of peak occurrences. The main processing steps are i) removing high-frequency components ii) squaring, iii) smoothing and iv) peak detection.

Removing high-frequency components

Since illumination peaks are byproducts of pedestrian movements, the frequency of their occurrences is determined both by luminary spacing and the speed. Pedestrian walking pace is around 2Hz with a stride length in the range of 0.6m – 0.8m. For example, in the information technology building (ITB) at McMaster the spacing between two neighboring luminaries in the corridor is around 2.5m. Thus, the time between two neighboring illumination peaks is roughly $\frac{2.5}{0.7\times 2} = 1.787s$ or 0.56Hz. Therefore, a low-pass filter can be applied to the input signal to remove high-frequency noise.

Let the cutoff frequency be f_c and $\omega_c = 2\pi f_c$. Clearly, the choice of the cutoff frequency is important, and it varies among individuals and environments. We leverage the self-tune adaptive LPF first suggested by Libby for step counting [18]. The cutoff frequency f_c can be chosen such that in the frequency domain a certain percentage (e.g., 90%) of energy falls below f_c.

Squaring

After LPF, the signal z_{lpf} is then squared to obtain $z_{sq}(t) = z_{lpf}(t)^2$. Squaring enhances large values more than small values, and thus makes peak detection easier.

Smoothing

Due to non-linearity of squaring, higher frequency components may be present in the resulting signal. An additional moving-window average (MWA) smoothing is applied as follows,

$$z_{mwa}(t) = \frac{z_{sq}(t-\frac{W}{2}+1)+\ldots+z_{sq}(t)+\ldots+z_{sq}(t+\frac{W}{2}-1)}{W}, \tag{10}$$

where $z_{sq}(t)$ is the output from the squaring step, z_{mwa} is the output waveform after the MWA, and W is the window size.

Peak detection

Lastly, we take the first-order derivative of $z_{mwa}(t)$. A sign change in the resulting waveform corresponds to a peak.

Figure 4 summarizes the steps for peak extraction and the input and output waveforms of each step. To this end, we obtain the binary observation o_t to be used in the SIR filter, where $o_t = 1$ and $o_t = 0$ indicate the presence of a peak or not at time t, respectively.

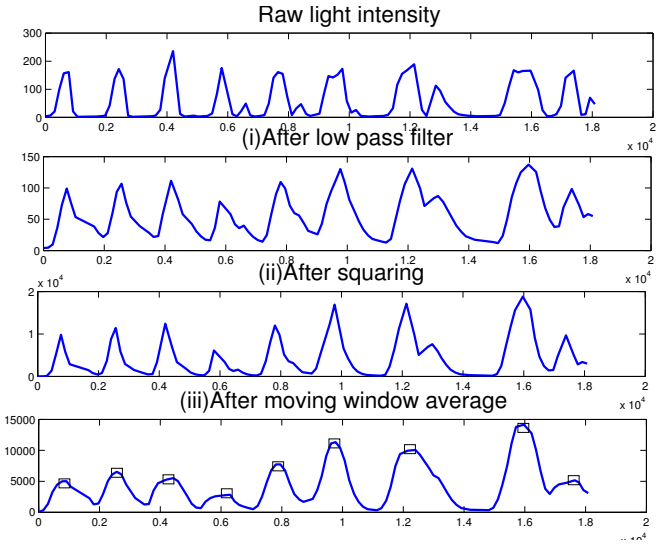

Figure 4. Illustration of Illumination Peak Detection

Selective observation model

Now, we are in the position to present the observation model based on illumination peaks. Luminary observations are selectively incorporated in particle filter updates when peak detection is deemed reliable.

Observation model

In contrast to RF signal strength, which only depends on the current position, the existence of an illumination peak depends on the current and the previous positions. Therefore, we rewrite the observation model as $p(o_t|\vec{s}_{t-1:t}, \mathscr{M}_l)$. Recall that $\mathscr{M}_l$ is the ground truth luminary placement map. In this work, we do not explicitly model map errors. However, the particle filter framework can be easily extended to account for

map errors if a probabilistic error model is given. A suitable observation model needs to account for peak detection errors in the procedure described in the previous section.

Define $\aleph : \mathbb{R}^2 \times \mathbb{R}^2 \times \mathbb{M} \to \{0,1\}$ a functional mapping from two locations to a binary indicator whether a (functioning) luminary exists between the two locations or not given the map. Let $\hbar : \mathbb{R}^2 \times \mathbb{R}^2 \times \mathbb{M} \to \mathbb{R}$ be a functional mapping from two locations to the Euclidean distance to the closest luminary (by taking the minimum distance between the two) given the map.

For any three-tuple $(s_t, s_{t-1}, \mathscr{M}_l)$, the following confusion matrix completely characterizes the observation model, where $p_f(\cdot)$ and $p_d(\cdot)$ are the probability of false alarm (False positive) and the probability of detection (True positive), respectively.

	$\aleph(s_t, s_{t-1}, \mathscr{M}_l) = 0$	$\aleph(s_t, s_{t-1}, \mathscr{M}_l) = 1$
$o_t = 0$	$1 - p_f(s_t, s_{t-1}, \mathscr{M}_l)$	$1 - p_d(s_t, s_{t-1}, \mathscr{M}_l)$
$o_t = 1$	$p_f(s_t, s_{t-1}, \mathscr{M}_l)$	$p_d(s_t, s_{t-1}, \mathscr{M}_l)$

Table 1. The Observation Model

From the experimental evaluation of the peak extraction procedure, we observe that both the false alarm rate and the probability of detection decrease as the user moves away from the luminary. As a result, we propose the following empirical model:

$$p_f = \varepsilon_1 \cdot \exp(-\hbar(\vec{s}_{t-1}, \vec{s}_t, \mathscr{M}_l)), \tag{11}$$

and

$$p_d = \varepsilon_2 \cdot \exp(-\hbar(\vec{s}_{t-1}, \vec{s}_t, \mathscr{M}_l)), \tag{12}$$

where ε_1 and ε_2 are constant factors. From empirical results, we find that $\varepsilon_2 > \varepsilon_1$.

Selective strategy

We observe through preliminary experiments that when making turns, the actual trajectories that users follow may vary a lot, e.g, along the far corner, along the near corner or cut through the corner, etc. As a result, luminaries close to the corner tend to be misdetected. Consequently, in the observation model, we only incorporate peak detection results when users' heading directions remain roughly the same. This is called the *selective observation model*. Turns can be reliably determined through variations in gyro readings (as illustrated in Figure 5).

MOTION ESTIMATION

Recall that the motion model $f_t(\vec{s}_t | \vec{s}_{t-1}, \mathscr{M})$ characterizes the relationship between the user locations at time $t-1$ and t. Let the displacement be l_t and the heading direction be θ_t (both are random variables at t) during the interval $[t-1, t]$. Then, if the transition from $\vec{s}_{t-1}$ to $\vec{s}_t$ is valid according to the map, we have

$$\vec{s}_t = \begin{pmatrix} x_t \\ y_t \end{pmatrix} = \begin{pmatrix} x_{t-1} + l_t cos(\theta_{t-1}) \\ y_{t-1} + l_t sin(\theta_{t-1}) \end{pmatrix}. \tag{13}$$

Therefore, the key in deriving the motion model is to determine the distribution of displacement and heading directions from the IMU measurements. We break it into three parts, namely, i) displacement estimation, ii) heading estimation, and iii) refined motion model with map constraints.

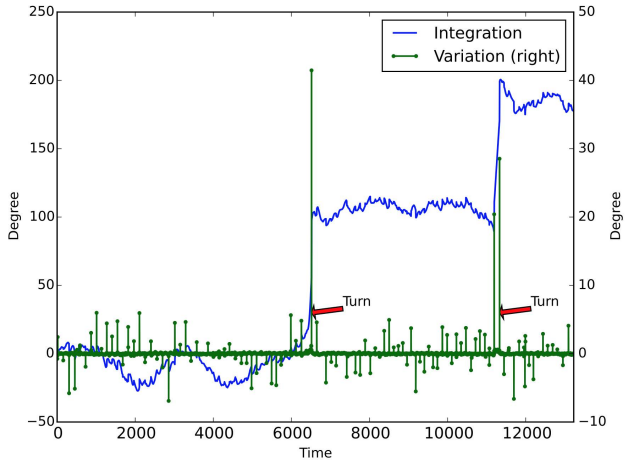

Figure 5. The Integration and Variation of Gyro Measurements

Displacement estimation

In PDR approaches, displacement is typically estimated through step counts and stride length estimation.

Step count

During one step cycle, a person's body goes through the "stance state" when the person has both of their feet on the ground, and the "swing state" when the person has only one foot on the ground. As gait is nearly periodic, steps can be detected by identifying peak horizontal or vertical acceleration.

Let the 3-axis accelerometer readings at time t be $acc_x(t), acc_y(t), acc_z(t)$. We first compute the magnitude $acc(t) = \sqrt{acc_x(t)^2 + acc_y(t)^2 + acc_z(t)^2}$. Similar to the peak illumination extraction, we apply LPF with an adaptive cutoff frequency, squaring, moving window averaging and peak detection to $acc(t)$. Each peak corresponds to one step.

Luminary-assisted stride length estimation

It has been reported in [16] that the stride length is roughly linear to the stride frequency f_{sl} as,

$$l_{sl} = a \cdot f_{sl} + b, \tag{14}$$

where a and b are constants determined by individual's anatomical features such as height. By taking the step frequency into account, this linear model allows the adaption of stride length to walking speed. However, as the constants a and b vary from person to person, it is non-trivial to decide their exact values [16]. Interestingly, we observe that the placement of luminaries can in fact be used to estimate for stride length. Given the distance of two neighboring luminaries $light_{i-1}$ and $light_i$ detected consecutively, and the (fractional) step counts n between these two luminaries, we can calculate the instantaneous stride length as:

$$l_{sl} = \frac{dist(light_{i-1}, light_i)}{n}. \tag{15}$$

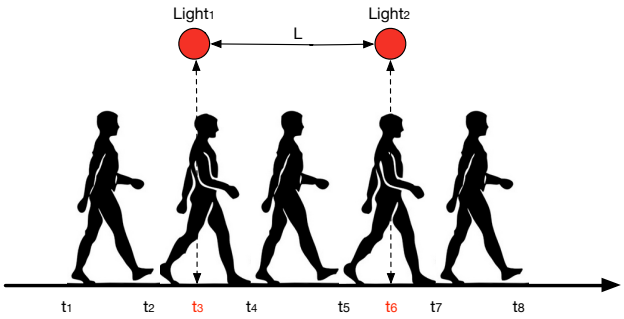

Figure 6. Luminary Detection-based Stride Length Estimation

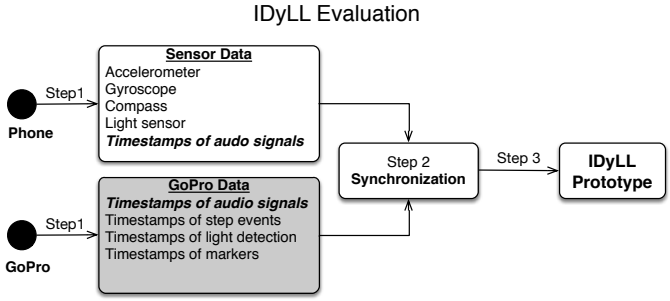

Figure 7. Evaluation Procedure

Clearly, due to the lack of identity information, we do not know exactly which luminaries have been detected. Instead, the id of the nearest luminary to the *estimated* location is used. Let $t^l_j, j = 1,\ldots,N$ and $t^s_i, i = 1,\ldots,K$ be the respective times that steps and luminaries are detected using the step and peak detection algorithms discussed earlier. Without loss of generality, we have $t^l_{i-2} < t^s_{j_1} < t^l_{i-1}$, $t^l_{i-1} < t^s_{j_1+1}, t^s_{j_2-1} < t^l_i$, and $t^l_i < t^s_{j_2} < t^l_{i+1}$. In other words, the onset of the j_1th step occurs between luminary $i-2$ and $i-1$, while the onset of the j_2-1th step occurs between luminary i and $i+1$. The fractional step count is then computed as,

$$n = \frac{t^s_{j_1+1} - t^l_{i-1}}{t^s_{j_1+1} - t^s_{j_1}} + \frac{t^l_i - t^s_{j_2-1}}{t^s_{j_2} - t^s_{j_2-1}} + (j_2 - j_1 - 2) \qquad (16)$$

As an example, in Figure 6, the timestamps of detected step and luminary events are $\{t_1,t_2,...,t_8\}$, where $\{t_1,t_2,t_4,t_5,t_7,t_8\}$ correspond to step events, and $\{t_3,t_6\}$ are illumination peak detection times. The fractional step count is $n = \frac{t_4-t_3}{t_4-t_2} + \frac{t_6-t_5}{t_7-t_5} + 1$. The instantaneous step length is thus estimated as $\frac{L}{n}$, where L is the distance between the two luminaries.

Velocity estimation

Though the step count algorithm can achieve high accuracy, it may still under- or over-count the steps, resulting in inaccurate displacement estimates. Furthermore, with step counts, the interval of location updates will be on the order of 0.5 to 1 second. To mitigate these problems, we calculate the average velocity with a time window of K steps when users are moving. Consider a K-step window $\{i_1,...,i_K\}$. Let the stride length of the j_{th} step be l_{sl,i_j}, and the start and end timestamp of the j_{th} step be t_{i_j} and t'_{i_j}. Then the velocity during the time window can be estimated as:

$$v_t = \frac{\sum_{j=1}^{K} l_{sl,i_j}}{t'_{i_K} - t_{i_1}}. \qquad (17)$$

Complementary filter based heading estimation

A compass sensor reports *Azimuth* (the compass bearing east of magnetic north). When a phone is facing up (as needed by light sensing and navigation), it is reasonable to assume that the phone attitude is constant, and the phone heading and the heading of the person are identical. Otherwise, we can adopt sophisticated methods for phone attitude estimation such as the one detailed in [25].

It is well known that compass readings are sensitive to magnetic disturbance in the environment. As a result, a compass may only give true readings occasionally. In contrast, gyroscopes measure rate of rotation, and can give accurate estimation of heading changes through continuous integration on angular velocities [35]. A complementary filter [27] can thus be used to combine the compass and gyro readings.

Let $\theta^{compass}$ be the heading estimation from compass and $\delta^{gyro}_{t-1,t}$ the change in heading estimated from gyro between time $t-1$ and t. The heading estimation θ_t at time t is thus given by,

$$\theta_t = c \cdot (\theta^{compass}_t) + (1-c) \cdot (\theta_{t-1} + \delta^{gyro}_{t-1,t}), \qquad (18)$$

where c is a small constant.

Refined motion model

Now, we are in the position to complete the refined motion model with map constraints. We first sample $\theta^{compass}_t$ from a Gaussian distribution $\mathcal{N}(\theta^{compass}_t, \sigma^2_\theta)$ given the measured heading direction $\theta^{compass}_t$ from the compass, and σ_θ is empirically determined. With with the angle variation from $t-1$ to t, $\delta^{gyro}_{t-1,t}$, the final heading is given by (18). From the velocity estimate v_t in (17), the displacement is given by $v_t \cdot (t_i - t_{i-1})$. From (13), we obtained $\vec{s}_t$. If the transition from $\vec{s}_{t-1}$ to $\vec{s}_t$ is invalid according to $\mathcal{M}_p$, $\vec{s}_t$ will be re-sampled until a valid next system state is obtained.

EXPERIMENTAL EVALUATION

We evaluate the performance of IDyLL in three different buildings in McMaster University with different luminary arrangements. We aim to answer the following questions: (a) How well can IDyLL locate users under different luminary arrangements, (b) How do the proposed motion model and observation model contribute to location accuracy, and (c) how well do the step detection and illumination peak detection algorithms work in real-world scenarios.

Experimental methodology

We have implemented IDyLL in Python for fast prototyping. Real-world data sets are collected from multiple walks in different buildings and are used in the evaluation.

We have implemented an Android app (Figure 8b), to collect data from accelerometer, compass, gyroscope and light sensor on smartphones. To obtain the ground truth location information during data collection, a GoPro camera is mounted on a helmet, as depicted in Figure 9a, and records the view from top down during the walks (Figure 9b). Several markers are placed on the floor along the walks in advance (See Figure 8a). To synchronize GoPro videos with the sensing data from the phone, audio cues (consisting of a sharp audible signal) are played back periodically by the mobile device during the experiments. The video is then post-processed to extract the time instances when the user passes individual markers. Since markers have known locations, the resulting timestamps can be used to evaluate the accuracy of the proposed algorithms.

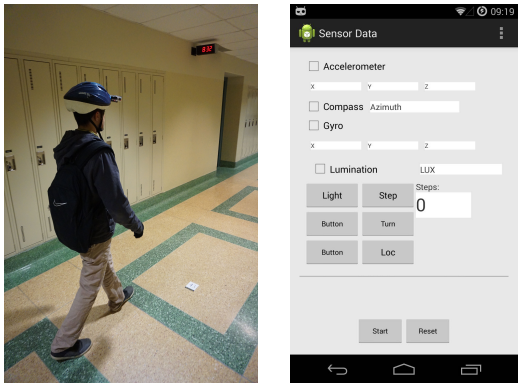

(a) Experiment Procedure (b) Data Collection

Figure 8. Android Apps Developed for Data Collection

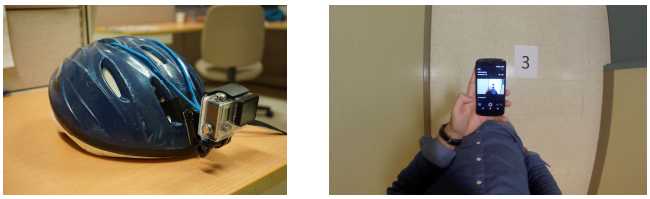

(a) Helmet with GoPro (b) The Video Screen Shot

Figure 9. GoPro Camera for Recording and a Snapshot of a Recorded Video

The work flow of evaluation is summarized in Figure 7. The parameters used in the implementation are given in Table 2.

Parameters	Value
Number of particles N	3000
Window size for light detection W	5 sample points
σ_θ	6.7°
$\varepsilon_1, \varepsilon_2$	0.7, 0.9
Time interval Δt	20 milliseconds

Table 2. Parameter Settings

Performance

Accuracy of step counts

Four rounds of experiments have been performed to evaluate the accuracy of step counting. As shown in Table 3, the average precision is 96% and average recall is 94%.

Test#	Total # of steps	TP	FP	FN	Precision	Recall
1	85	80	2	5	0.976	0.941
2	85	78	3	7	0.963	0.918
3	84	83	0	1	1	0.988
4	85	77	5	8	0.939	0.906
Avg Precision: 96%, Avg Recall: 94%						

Table 3. Performance of Step Counting

Accuracy of peak illumination detection

We choose a trajectory along the corridor to evaluate the performance of the luminary detection module in IDyLL. There are a total of 70 luminaries along the trajectory. Four rounds of experiments are performed. As shown in Table 4 , the average precision of luminary detection is 95%, and the average recall is 92%.

Test#	Total # of luminaries	TP	FP	FN	Precision	Recall
1	70	65	1	5	0.985	0.929
2	70	66	2	4	0.971	0.943
3	70	62	6	8	0.912	0.886
4	70	65	5	5	0.929	0.929
Avg Precision: 95%, Avg Recall: 92%						

Table 4. Performance of Illumination Peak Detection

Location accuracy

Three floors of different buildings with different luminary arrangements on McMaster University campus were selected to evaluate the performance of IDyLL. They are the second floor of Information Technology Building (ITB-2F), the second floor of AN Bourns Science Building (ABB-2F) and the third floor of Student Center (SC-3F). The first two are typical academic buildings, as depicted in Figure 10. The third one corresponds to an open area in a recreation center. Respectively, there are 57, 42 and 21 luminaries in these test areas.

The initial position is assumed to be known. To evaluate the performance of IDyLL in details, five different solutions have been compared. The detailed algorithms are specified in Table 5. The first is a baseline PDR approach (denoted as Sol_1). This solution only makes use of IMU measurements along with map constraints. It takes step frequency into account when estimating stride length. IDyLL is the final solution incorporating all components. The remaining three algorithms serve to evaluate the contribution of individual component techniques of IDyLL (namely, velocity based motion model, luminary assisted stride length estimation, luminary observation model, and selective luminary observation).

Figure 11 shows the average location accuracy for all methods in three buildings. We find that IDyLL can achieve sub-meter

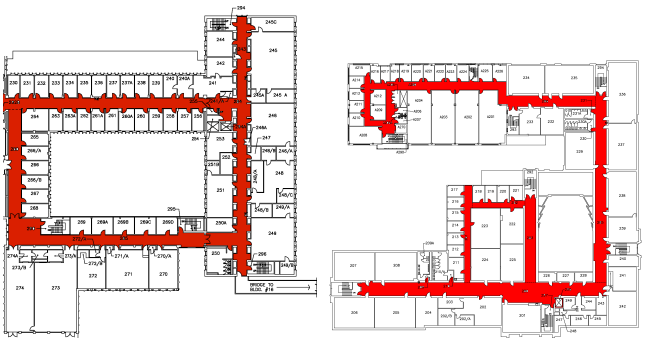

(a) ABB-2F (b) ITB-2F

Figure 10. Floor Maps of Test Areas in Two Buildings

Name	Sol_1	Sol_2	Sol_3	Sol_4	*IDyLL*
Particle filter	√	√	√	√	√
New motion model	×	√	√	√	√
Step frequency	√	√	√	√	√
Light-assisted stride length	×	√	×	√	√
Light observation	×	×	√	√	√
Selective strategy	×	×	×	×	√

Table 5. Summary of the Five Different Solutions Evaluated

location accuracy (0.38 m, 0.42 m, and 0.74 m) in different buildings with different luminary arrangements. Significant performance gains over the baseline PDR method is accomplished by combining all components. Both Sol_2 and Sol_3 utilize luminary information but in two different ways. Specifically, Sol_3 uses illumination peaks to obtain more accurate stride length estimation, while Sol_2 incorporates illumination peaks in the observation model. The experiment results show that either way leads to significant reductions in location errors under all settings, and in fact the two approaches are complementary to each other as evident in the further improved performance of Sol_4, which combines both approaches. To this end, we could reasonably conclude that utilizing conventional luminary information, even in absence of identity and low sampling rates of smart phone photodiodes, can indeed improve indoor localization accuracy.

Understandably, average performance does not tell the whole story. Large spurious errors can be particularly harmful to LBS. Figure 12 shows the location error over one walk of length 140 meters in ITB-2F. We observe that approaches that utilize luminary information consistently outperform the baseline PDR method. The worst case for Sol_1 happens because during the execution of the algorithm all particles are removed and the Particle Filter algorithm needs to reinitialize all the particles. When comparing the performance of Sol_4 and IDyLL in Figure 12, we find that Sol_4 in some cases has location errors between 2 - 4 meters (e.g., between distance 60 - 70 and around distance 120). This is also evident from Figure 13, which shows the cumulative density function (CDF) of different algorithms along different trajectories over multiple runs. A jump can be observed for Sol_4 around 2 meters (and to a much lesser extent in IDyLL). This in fact corresponds to the inter-luminary distance around 2 meters. In other words, large errors in Sol_4 can be attributed to mis-location between

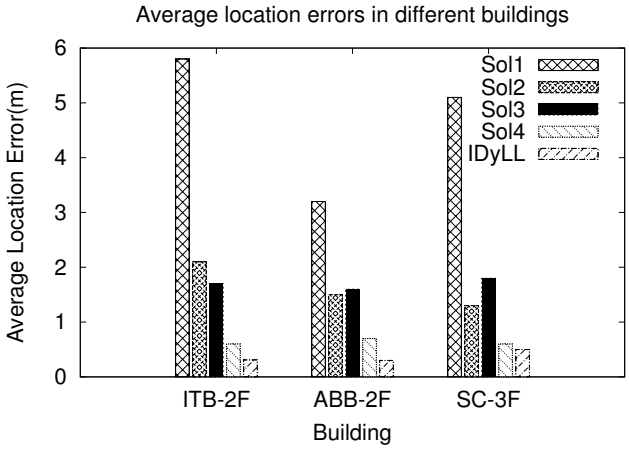

Figure 11. Performance Comparison in Different Buildings

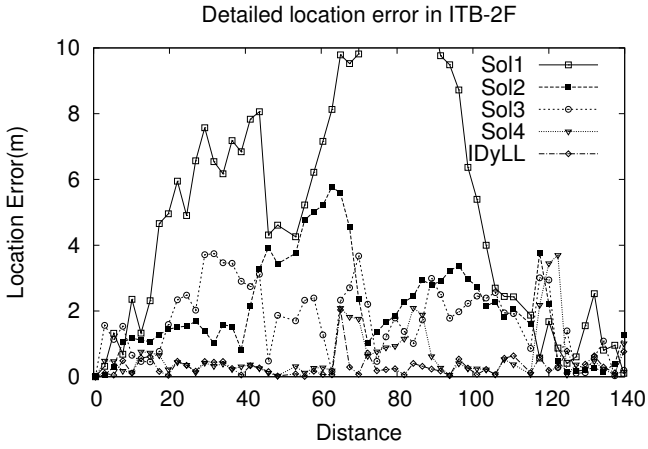

Figure 12. Location Errors over Distance in ITB-2F

Solution	Avg Error(m)	75%ile	90%ile
Sol_1	5.8	8.1	12.1
Sol_2	2.1	2.9	4.1
Sol_3	1.7	2.4	3.1
Sol_4	0.6	0.7	1.8
IDyLL	0.38	0.5	0.6

Table 6. 50%, 70% and 90%ile Location Errors

neighboring luminaries. This is essentially due to the lack of luminary identities with conventional luminaries. However, in IDyLL, by excluding luminary observations when users make turns, we can significantly reduce occurrence of such errors.

Table 6 summarizes the 50, 75 and 90 quantiles of location errors using five solutions. We find that despite luminary identity ambiguity, the mean and 90 percentile location errors of IDyLL are significantly less than those with the baseline algorithm.

A Qualitative Comparison with Representative IPS

The absence of publicly available source codes and detailed parameter settings make it challenging to provide an objec-

System	Modalities	Face-Up	Method	Map	Reported Average Error
Zee[23]	Accelerometer, Gyro, Compass, Received Signal Strength (RSS)	No	PDR & Fingerprinting-based	Yes	1.2m
LiFS[31]	Accelerometer, RSS	No	Fingerprinting-based	Yes	5.88m
RADAR[3]	RSS	No	Fingerprinting-based	Yes	2.94m
SAIL[20]	Accelerometer, Gyro, Compass, Channel State Information (CSI), WLAN Time-of-Flight (ToF)	No	PDR & others	Yes	0.8m
Epsilon[17]	Modulated LED	Yes	Beacon-based (VLC)	No	0.4m
IDyLL	Accelerometer, Gyro, Compass, Conventional Luminaries	Yes	PDR & others	Yes	0.5m

Table 7. Comparison between IDyLL and Other Systems

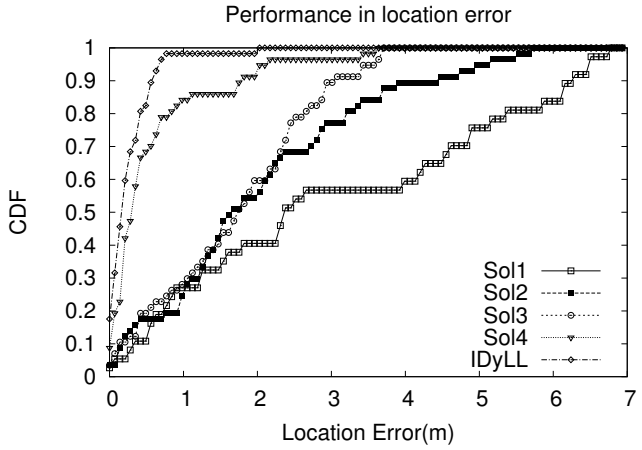

Figure 13. Cumulative Distribution Function of Location Errors

tive quantitative comparison against existing IPS. Instead, we summarize the key differences between IDyLL and existing schemes along the line of sensing modality, location method, additional requirements (e.g, whether phones need to be face-up, and whether indoor maps are required), and reported average location error. Table 7 gives a qualitative comparison among Zee[23], LiFS[31], RADAR[3], SAIL[20], Epsilon[17] and IDyLL. Note that the list is far from being exhaustive. However, we feel these systems are representative of their respective categories in terms of sensing modalities used.

LIMITATIONS

In this section, we discuss the main limitations of IDyLL. IDyLL is designed under the premise that there exist persistent and detectable variations in lighting patterns over space. We acknowledge that this may not be always true in situations such as homogeneous indoor lighting, luminaries too high up in the ceiling or strong sunlight from outside. Furthermore, the use of ambient illumination makes IDyLL sensitive to environmental interference such as, shadowing from furniture, the user's body, or other users in the space. Illumination peaks due to changes of the device's orientation could also result in false alarms in luminary detection. However, as demonstrated through the selective observation model in IDyLL, in these situations, we could turn off components of IDyLL and fall back to the base PDR approach.

In the current implementation, we assume floor map $\mathscr{M}_p$ and luminary placement map $\mathscr{M}_l$ are available and accurate. During data collection we have indeed observed luminary burnouts and the particle filter framework was shown to be able to handle such situations to some extent. The absence of accurate luminary position information may compromise the applicability of IDyLL. In [30], we have devised a mechanism to infer luminary burn-out with only crude indoor position information. It is expected that combining this technique with IDyLL can improve the robustness of the latter.

The need for face-up attitude of the phone is another limitation of IDyLL. This is true for most visible light based approaches. It may not be a serious constraint when people wear smart glasses or hold phones up to view indoor maps during navigation.

Finally, the computational cost of IDyLL scales with the number of particles utilized rendering the current implementation not suitable for battery-powered wearable devices with limited computation capabilities. Further improvement of the robustness and reduction of the computation and energy costs of IDyLL will be part of our future work.

CONCLUSION AND FUTURE WORK

In this paper, we have presented IDyLL, a system that leverages a previously under-utilized source of information – luminaries in indoor spaces, for localization. IDyLL does not require modification to existing light infrastructure or end user devices. Experimental evaluation shows that it can achieve significant reduction in localization errors compared to PDR approaches using only IMU sensors.

As future work, we will continue to improve the robustness and accuracy of IDyLL. We will also investigate incremental deployment of modulated luminaries and incorporation of other sensing modalities for location fixes.

ACKNOWLEDGMENTS

The authors would like to thank Eric Edwards for helpful discussions. The work is in part supported by National Science and Engineering Council of Canada under Discovery Grant and Ontario Center of Excellence.

REFERENCES

1. 2014. Location-Based Services Reports. (2014). Accessed: 2014-7-29 from http://www.pewinternet.org/2013/09/12/location-based-services/.

2. Klaithem Al Nuaimi and Hesham Kamel. 2011. A survey of indoor positioning systems and algorithms. In *Innovations in Information Technology (IIT), 2011 International Conference on*. IEEE, 185–190.
3. Paramvir Bahl and Venkata N Padmanabhan. 2000. RADAR: An in-building RF-based user location and tracking system. In *INFOCOM 2000. Nineteenth Annual Joint Conference of the IEEE Computer and Communications Societies. Proceedings on*, Vol. 2. IEEE, 775–784.
4. Mehmet Bilgi, Murat Yuksel, and Nezih Pala. 2010. 3D optical wireless localization. In *GLOBECOM Workshops (GC Wkshps)*. IEEE, 1062–1066.
5. Pavel Davidson, Jussi Collin, and Jarmo Takala. 2010. Application of particle filters for indoor positioning using floor plans. In *Ubiquitous Positioning Indoor Navigation and Location Based Service (UPINLBS), 2010*. IEEE, 1–4.
6. Arnaud Doucet, Nando De Freitas, and Neil Gordon. 2001. An introduction to sequential Monte Carlo methods. In *Sequential Monte Carlo methods in practice*. Springer, 3–14.
7. Arnaud Doucet and Adam M Johansen. 2009. A tutorial on particle filtering and smoothing: Fifteen years later. *Handbook of Nonlinear Filtering* 12 (2009), 656–704.
8. Andrew R Golding and Neal Lesh. 1999. Indoor navigation using a diverse set of cheap, wearable sensors. In *Wearable Computers, The Third International Symposium on*. IEEE, 29–36.
9. Fredrik Gustafsson. 2010. Particle filter theory and practice with positioning applications. *IEEE Aerospace and Electronic Systems Magazine* 25, 7 (July 2010), 53–82. DOI: http://dx.doi.org/10.1109/MAES.2010.5546308
10. Robert Harle. 2013. A survey of indoor inertial positioning systems for pedestrians. *IEEE Communications Surveys and Tutorials* 15, 3 (2013), 1281–1293.
11. Pan Hu, Liqun Li, Chunyi Peng, Guobin Shen, and Feng Zhao. 2013. Pharos: Enable physical analytics through visible light based indoor localization. In *Proceedings of the Twelfth ACM Workshop on Hot Topics in Networks*. ACM, 5.
12. Antonio R Jimenez, Francisco Zampella, and Fernando Seco. 2013. Light-matching: a new signal of opportunity for pedestrian indoor navigation. In *Indoor Positioning and Indoor Navigation (IPIN), 2013 International Conference on*. IEEE, 1–10.
13. Soo-Yong Jung, Chang-Kuk Choi, Sang Hu Heo, Seong Ro Lee, and Chang-Soo Park. 2013. Received signal strength ratio based optical wireless indoor localization using light emitting diodes for illumination. In *Consumer Electronics (ICCE), 2013 IEEE International Conference on*. 63–64. DOI: http://dx.doi.org/10.1109/ICCE.2013.6486796
14. Incheol Kim, Eunmi Choi, and Huikyung Oh. 2012. Indoor User Tracking with Particle Filter. In *COGNITIVE 2012, The Fourth International Conference on Advanced Cognitive Technologies and Applications*. 59–62.
15. Nisarg Kothari, Balajee Kannan, Evan D. Glasgwow, and M. Bernardine Dias. 2012. Robust Indoor Localization on a Commercial Smart Phone. *Procedia Computer Science* 10, RoboSense (Jan. 2012), 1114–1120. DOI: http://dx.doi.org/10.1016/j.procs.2012.06.158
16. Fan Li, Chunshui Zhao, Guanzhong Ding, Jian Gong, Chenxing Liu, and Feng Zhao. 2012. A reliable and accurate indoor localization method using phone inertial sensors. In *Proceedings of the 2012 ACM Conference on Ubiquitous Computing - UbiComp '12*. ACM Press, New York, USA, 421. DOI: http://dx.doi.org/10.1145/2370216.2370280
17. Liqun Li, Pan Hu, Chunyi Peng, Guobin Shen, and Feng Zhao. 2014. Epsilon: A visible light based positioning system. In *11th USENIX Symposium on Networked Systems Design and Implementation (NSDI 14)*. USENIX Association, 331–343.
18. Ryan Libby. 2012. A Simple Method for Reliable Footstep Detection in Embedded Sensor Platforms. (2012).
19. Kaikai Liu, Xinxin Liu, and Xiaolin Li. 2013. Guoguo: Enabling fine-grained indoor localization via smartphone. In *Proceeding of the 11th annual international conference on Mobile systems, applications, and services*. ACM, 235–248.
20. Alex T. Mariakakis, Souvik Sen, Jeongkeun Lee, and Kyu-Han Kim. 2014. SAIL: Single Access Point-based Indoor Localization. In *Proceedings of the 12th Annual International Conference on Mobile Systems, Applications, and Services (MobiSys '14)*. ACM, New York, NY, USA, 315–328. DOI: http://dx.doi.org/10.1145/2594368.2594393
21. Chunyi Peng, Guobin Shen, Yongguang Zhang, Yanlin Li, and Kun Tan. 2007. Beepbeep: a high accuracy acoustic ranging system using cots mobile devices. In *Proceedings of the 5th international conference on Embedded networked sensor systems*. ACM, 1–14.
22. Gregary B Prince and Thomas DC Little. 2012. A two phase hybrid RSS/AoA algorithm for indoor device localization using visible light. In *Global Communications Conference (GLOBECOM)*. IEEE, 3347–3352.
23. Anshul Rai, Krishna Kant Chintalapudi, Venkata N Padmanabhan, and Rijurekha Sen. 2012. Zee: zero-effort crowdsourcing for indoor localization. In *Proceedings of the 18th annual international conference on Mobile computing and networking*. ACM, 293–304.

24. Nishkam Ravi and Liviu Iftode. 2007. Fiatlux: Fingerprinting rooms using light intensity. In *Pervasive Computing, Adjunct Proceedings of the Fifth International Conference on*.
25. Nirupam Roy, He Wang, and Romit Roy Choudhury. 2014. I am a smartphone and I can tell my user's walking direction. *Proceedings of the 12th annual international conference on Mobile systems, applications, and services - MobiSys '14* (2014), 329–342. DOI: http://dx.doi.org/10.1145/2594368.2594392
26. Chinnapat Sertthin, Emiko Tsuji, Masao Nakagawa, Shigeru Kuwano, and Kazuji Watanabe. 2009. A switching estimated receiver position scheme for visible light based indoor positioning system. In *Wireless Pervasive Computing, 2009. ISWPC 2009. 4th International Symposium on*. IEEE, 1–5.
27. Yangzhu Wang, Ning Li, Xi Chen, and Miao Liu. 2014. Design and Implementation of an AHRS Based on MEMS Sensors and Complementary Filtering. *Advances in Mechanical Engineering* 2014 (2014), 1–11. DOI: http://dx.doi.org/10.1155/2014/214726
28. Allen Jong-Woei Whang, Yi-Yung Chen, and Yuan-Ting Teng. 2009. Designing uniform illumination systems by surface-tailored lens and configurations of LED arrays. *Journal of display technology* 5, 3 (2009), 94–103.
29. Jie Xiong and Kyle Jamieson. 2013. ArrayTrack: A Fine-Grained Indoor Location System. In *NSDI*. 71–84.
30. Qiang Xu and Rong Zheng. 2015. Automated Detection of Burned-out Luminaries Using Indoor Positioning. In *IPIN 2015 Sixth International Conference on Indoor Positioning and Indoor Navigation (IPIN 2015)*. Banff, Canada.
31. Zheng Yang, Chenshu Wu, and Yunhao Liu. 2012. Locating in fingerprint space: wireless indoor localization with little human intervention. In *Proceedings of the 18th annual international conference on Mobile computing and networking*. ACM, 269–280.
32. Masaki Yoshino, Shinichiro Haruyama, and Masao Nakagawa. 2008. High-accuracy positioning system using visible LED lights and image sensor. In *Radio and Wireless Symposium*. IEEE, 439–442.
33. Paul A Zandbergen. 2009. Accuracy of iPhone locations: A comparison of assisted GPS, WiFi and cellular positioning. *Transactions in GIS* 13, s1 (2009), 5–25.
34. W. Zhang and M. Kavehrad. 2012. A 2D indoor localization system based on visible light LED. In *Photonics Society Summer Topical Meeting Series*. IEEE, 80–81. DOI: http://dx.doi.org/10.1109/PHOSST.2012.6280711
35. Pengfei Zhou, Mo Li, and Guobin Shen. 2014. Use it free: Instantly knowing your phone attitude. In *Proceedings of the 20th annual international conference on Mobile computing and networking*. ACM, 605–616.
36. Soumaya Zirari, Philippe Canalda, and François Spies. 2010. WiFi GPS based combined positioning algorithm. In *Wireless Communications, Networking and Information Security (WCNIS), 2010 IEEE International Conference on*. IEEE, 684–688.